ELSEVIER

Journal of Non-Crystalline Solids 235–237 (1998) 753–760

JOURNAL OF NON-CRYSTALLINE SOLIDS

Non-Debye conductivity relaxation in the non-Arrhenius $Li_{0.5}La_{0.5}TiO_3$ fast ionic conductor. A nuclear magnetic resonance and complex impedance study

C. León [a], J. Santamaría [a,*], M.A. París [b], J. Sanz [b], J. Ibarra [c], A. Várez [d]

[a] *Departamento de Física Aplicada III, Facultad de Ciencias Físicas, Universidad Complutense de Madrid, Avda, Complutense s/n, 28040 Madrid, Spain*

[b] *Instituto de Ciencia de Materiales de Madrid (CSIC), Cantoblanco, 28049 Madrid, Spain*

[c] *División de Estudios Superiores (CIDEMAC), Universidad Autónoma de Nuevo León, Guerrero y Progreso s/n, Monterrey, Nuevo León, Mexico*

[d] *Departamento de Ingeniería, Escuela Politécnica Superior, Universidad Carlos III de Madrid, 28911 Leganés, Spain*

Abstract

An analysis of electrical conductivity relaxation and nuclear magnetic resonance spin-lattice relaxation has been conducted to study the dynamics of the ionic diffusion process in the crystalline ionic conductor $Li_{0.5}La_{0.5}TiO_3$. Dc conductivity shows a non-Arrhenius temperature dependence, similar to the one recently reported for some ionic conducting glasses. Taking into account this non-Arrhenius dependence for the relaxation times, spin-lattice and conductivity relaxations are compared in the same frequency and temperature ranges. A single "stretched exponential" relaxation function of the form $f(t) = \exp(-(t/\tau)^{\beta})$, with $\beta = 0.4$, can be used to describe both relaxation processes in which correlation times differ in the preexponential factor.

PACS: 66.10.Ed

1. Introduction

Interest in the dynamics of the conduction process of fast ionic conductors has increased in recent years. Ion–ion interactions have been proposed to play an important role in ion diffusion, and an effort has been given to understanding its effect on the ion conduction process, particularly in glassy ionic conductors. In this context, nuclear magnetic resonance (NMR) spin-lattice relaxation (SLR) and electrical conductivity relaxation (ECR) measurements have been proposed as useful tools to study the effect of correlations in the ionic conduction process [1,2]. It is usual that the relaxation functions describing either SLR or ECR in fast ionic conductors deviate from the simple exponential dependence characteristic of ideal Bloembergen–Purcell–Pound (BPP) or Debye-like relaxations. The relaxation can be described using stretched exponentials of the Kohlrausch–Williams–Watts (KWW) form [3], $f(t) = \exp(-(t/\tau)^{\beta})$. Several models, such as the coupling model [4,5], diffusion-controlled model [6,7] or the jump relaxation model [8], have been proposed to explain the "non-exponentiality" observed in both relaxations. Nevertheless, it is still not known

* Corresponding author. Tel.: 34 91 3944435; fax: 34 91 3945 196; e-mail: jacsan@eucmax.sim.ucm.es.

0022-3093/98/$19.00
PII: S0022-3093(98)00626-7

whether the parameters defining the relaxation functions (relaxation times, τ, the exponent, β, and the activation energies for the ionic motion), obtained from ECR and from SLR, should be the same. Differences between the parameters obtained for the description of both processes have been previously predicted from Monte Carlo simulations of ionic motion in a disordered media [9], and these theoretical results seem to agree qualitatively with experimental discrepancies reported by different authors for both relaxations in glassy systems [1,2,10,11].

It has been shown recently that many ionic conducting glasses, with chemistry and composition optimized to obtain larger electrical conductivities, present another interesting feature: their dc conductivity has a non-Arrhenius temperature dependence. Kincs and Martin [12] have described this behavior as a general feature of these materials, and Ngai and Rizos [13] have proposed an explanation which points to ion–ion correlation, or more precisely a decrease in the relaxation rate due to correlation effects among ions, as the reason for this non-Arrhenius dependence.

In this paper we present a comparative analysis of the results obtained from NMR and electrical conductivity measurements on a crystalline ion conductor, $Li_{0.5}La_{0.5}TiO_3$, which has one of the largest conductivities of lithium conducting crystalline materials [14–17]. We show that both relaxation processes can be described with KWW functions with the same β exponent and equally activated relaxation times. Interestingly, the temperature dependence of the conductivity shows a non-Arrhenius dependence similar to that found in glassy systems [12], suggesting that this feature could be more general and not only restricted to ionic conducting glasses.

2. Experimental

Samples were prepared by heating a stoichiometric mixture of Li_2CO_3, La_2O_3 and TiO_2 reagents at 1200°C. The reacted powder was pelleted and fired at 1350°C in air for several hours (5–11 h) and then quenched to room temperature. The metal molar ratio was determined by inductively coupled plasma spectroscopy (ICP) using a spectrometer (JY-70 PLUS). The tetragonal perovskite structure, space group *P4mm*, was verified by X ray and electron diffraction. The ^{7}Li NMR spin-lattice relaxation times (T_1) were measured with a spectrometer (SXP 4/100 Bruker). Determination of T_1s at each temperature was done by using the classical $\pi - \tau - \pi/2$ sequence [18]. The frequencies used were 31, 20 and 10.6 MHz and the experiments were carried out between 100 and 500 K. Admittance spectroscopy was measured in the frequency range 20 Hz–30 MHz using automatically controlled precision LCR meters (HP 4284A and HP 4285A), at temperatures between 150 and 500 K. The samples were cylindrical pellets 5 mm in diameter and 0.7 mm thick on whose faces gold electrodes were deposited by evaporation. Measurements were conducted under a N_2 flow to ensure an inert atmosphere.

3. Results and discussion

3.1. Electrical conductivity relaxation

The frequency dependence of the real part of the conductivity is presented in Fig. 1. Conductivity has a low frequency plateau and a crossover to a power law dependence at higher frequencies. This behavior, characteristic of ion hopping, can be described according to a complex conductivity $\sigma^*(\omega)$ of the form

$$\sigma^*(\omega) = \sigma_{dc}[1 + (i\omega/\omega_p)^n], \quad (1)$$

where σ_{dc} is the dc conductivity, ω_p is a crossover frequency and the exponent, $n \approx 0.6$, is related to the degree of correlation among moving ions. The crossover frequency, ω_p, has the same temperature dependence as σ_{dc}, and in fact, the relation $\omega_p = \sigma_{dc}/\varepsilon_\infty$ holds [19], where ε_∞ is the high frequency permittivity. ε_∞ has been obtained from the high frequency capacitance, and shows a linear temperature dependence according to $\varepsilon_\infty = 1.75 \times 10^{-10} + 3.15 \times 10^{-12}\ T$ F/m. The decrease observed for the conductivity at lower frequencies and higher temperatures is due to blocking of ions at grain boundaries, but these blocking effects do not affect the analysis on the frequency depen-

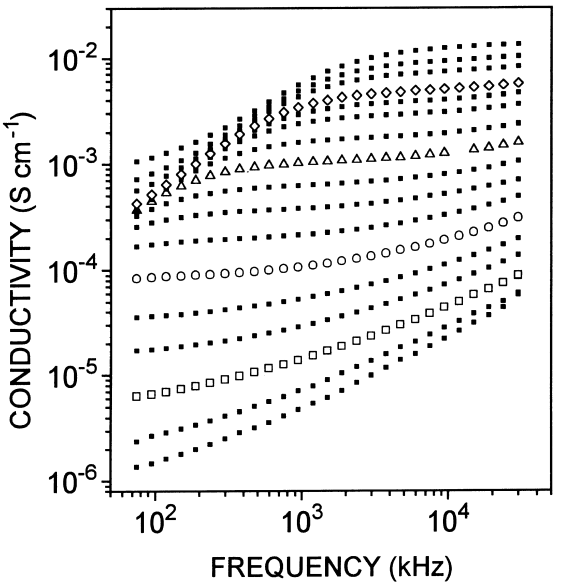

Fig. 1. Real part of the conductivity vs. frequency at several temperatures (200–500 K). Open symbols are data at 225 K (□), 271 K (○), 338 K (△) and 407 K (◇).

dence of the bulk conductivity in terms of expression (1).

The dispersion of the conductivity in the frequency domain according to expression (1) can be alternatively interpreted in terms of a KWW relaxation function, $\phi(t)$ in the time domain, which takes the form of a stretched exponential,

$$\phi(t) = \exp(-(t/\tau_\sigma)^{\beta_\sigma}), \tag{2}$$

with τ_σ as a temperature dependent relaxation time, inversely proportional to the dc conductivity, and $\beta_\sigma = 1 - n$. Although expressions (1) and (2) cannot be obtained analytically from each other, both can be used to get an empirical description of the relaxation process in the frequency and time domain [20]. The electric modulus can be expressed as a function of the time derivative of the ECR relaxation function, providing a connection between both representations:

$$M^*(\omega) = \frac{1}{\varepsilon_\infty}\left[1 - \int_0^\infty \left(-\frac{\mathrm{d}\phi}{\mathrm{d}t}\right) \mathrm{e}^{-\mathrm{i}\omega t}\,\mathrm{d}t\right], \tag{3}$$

which allows determining the relaxation function in the time domain from experimental data measured in the frequency domain. Nearly temperature independent β_σs close to 0.4 have been obtained [17], confirming the relationship $\beta_\sigma = 1 - n$.

Dc conductivity data have been obtained from conductivity vs frequency plots fitting to expression (1), and from the parameters obtained for the KWW function through the equation $\sigma_{\mathrm{dc}} = \varepsilon_\infty(\beta_\sigma/(\Gamma(1/\beta_\sigma)\tau_\sigma))$ [5], and then plotted in Fig. 2 in an Arrhenius fashion. The temperature dependence of the dc conductivity over the whole temperature range is clearly non-Arrhenius, but Arrhenius local fits of the form $\sigma_{\mathrm{dc}} = \sigma_\infty \exp(-E_\sigma/kT)$ yield activation energies, E_σ, of 0.4 eV at low temperatures and 0.26 eV in the high temperature range.

The complex electric modulus is related to the Fourier transform of the time derivative of the ECR relaxation function ($\hat{\Phi}(\omega)$) as quoted by expression (3), which can be rewritten as

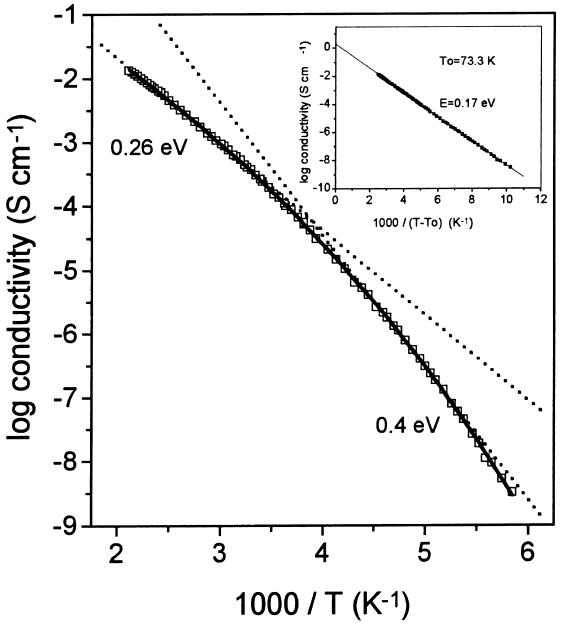

Fig. 2. DC conductivity vs. $1000/T$ showing a strongly non-Arrhenius behavior. Dashed lines are Arrhenius local fits in temperature ranges where activation energies are calculated in $1/T_1$ plots. Activation energies of 0.4 and 0.26 are obtained. Solid line is a fitting to a Vogel–Fulcher–Tamman function ($\sigma_{\mathrm{dc}} = \sigma_\infty \exp[-A/(T - T_K)]$) with $A = 1990$ K and $T_K = 73.3$ K. Dc conductivity vs. $1000/(T - 73.3)$ is also shown in an inset, stressing the goodness of this VFT fit.

$M^*(\omega) = (1 + \hat{\tilde{\Phi}}(\omega))/\varepsilon_\infty$. Using $\hat{\tilde{\Phi}}(\omega) = j\omega\hat{\Phi}(\omega) - 1$ and the expression $M^*(\omega) = j\omega Z^*(\omega) = j\omega/(\sigma^*(\omega) + j\omega\varepsilon_\infty)$ for the electric modulus, the complex impedance, $Z^*(\omega)$, is directly related to the Fourier transform of the relaxation function through $\hat{\Phi}(\omega) = \varepsilon_\infty Z^*(\omega)$. The temperature dependence of the real part of the complex impedance is presented in Fig. 3 at several frequencies. We can analyze from this figure the frequency and temperature dependences of the real part of $\hat{\Phi}(\omega)$, which will be useful later to compare ECR and SLR correlation functions provided that the NMR spectral density function is the Fourier transform of the SLR correlation function. $Z'(\omega_0, T)$ is represented in a logarithmic scale vs. $1000/T$, showing asymmetric peaks with maxima occurring at different temperatures for each frequency. All data points at different frequencies collapse in a single curve at the high temperature side of the peaks, because the relation $Z'(\omega_0, T) = 1/\sigma_{dc}(T)$ holds at the higher temperatures. Solid line in Fig. 3 represents the inverse of dc conductivity data presented in Fig. 2. These data have the non-Arrhenius temperature dependence of dc conductivity. β_σ, the exponent which characterizes the non-exponential ECR relaxation function, can be obtained from the frequency dependence of the impedance at the low temperature side of the peaks: at a fixed temperature the relation $Z'(\omega, T_0) \propto \omega^{-(1+\beta\sigma)}$ holds, and $\beta_\sigma = 0.4$ is obtained (see Fig. 4).

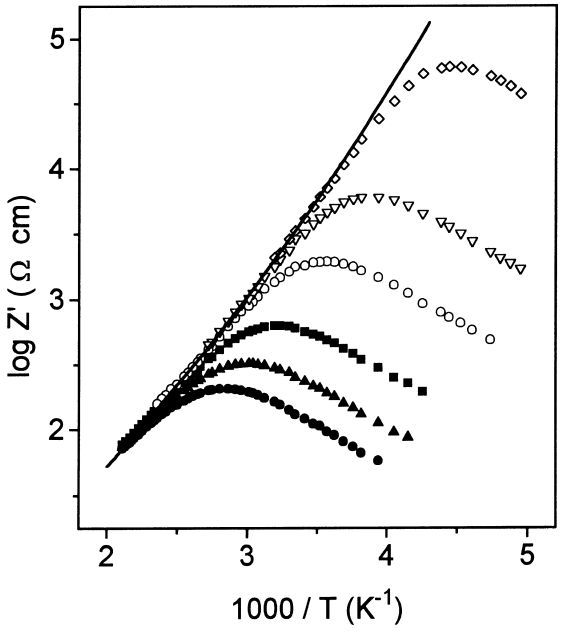

Fig. 3. Temperature dependence of the real part of the impedance, Z', at different frequencies (100 kHz (◇), 1 MHz (▽), 3 MHz (○), 10 MHz (■), 20 MHz (▲), 30 MHz (●)). Solid line represents the inverse of dc conductivity data presented in Fig. 2, which clearly shows the non-Arrhenius temperature dependence.

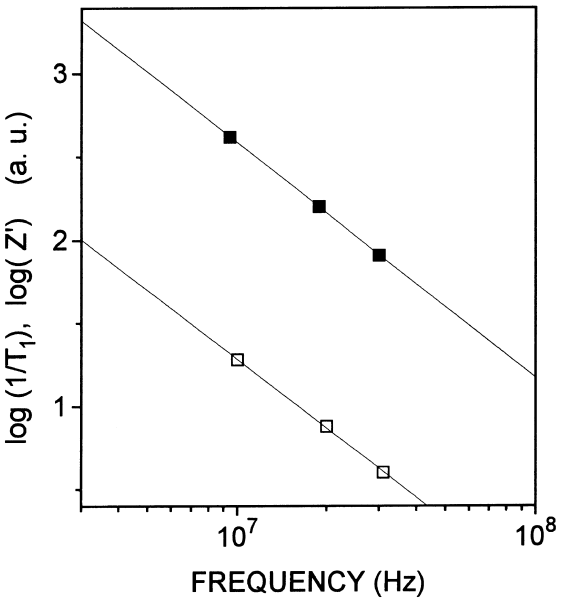

Fig. 4. Double logarithmic plot of the real part of the impedance (■), at $T = 254$ K, vs. measuring frequency, and of $1/T_1$ (□), at $T = 200$ K, vs. Larmor frequency. Straight lines are fits according to a KWW behavior of ECR and SLR with $\beta_\sigma = 0.41 \pm 0.02$ and $\beta_s = 0.38 \pm 0.02$, respectively.

3.2. Nuclear magnetic resonance

The static ^{7}Li NMR spectra ($I = 3/2$), recorded at increasing temperatures (Fig. 5), show only one line centered at the Li resonance frequency, whose width decreases as temperature increases. In these spectra, the (1/2,3/2) transitions produced by the quadrupole interaction of Li with its environment are not detected. To exclude the presence of broad masked satellite peaks associated with these transitions, the spectrum was recorded with a short excitation pulse (non-selective excitation)

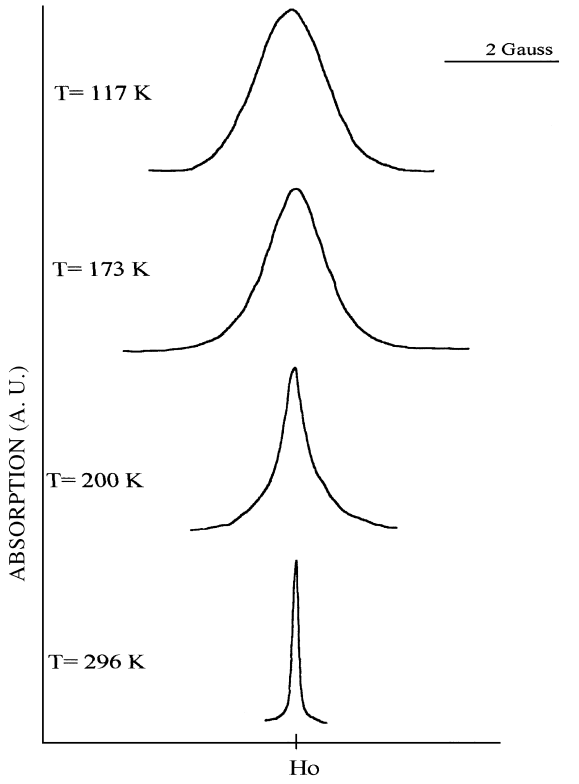

Fig. 5. Temperature dependence of the static ^{7}Li NMR spectra recorded at 31 MHz.

and the magic angle spinning (MAS) technique [17]. The absence of outer transitions was thus confirmed, concluding that lithium must occupy sites with small static quadrupole interaction, i. e., high symmetry sites.

At temperatures below 200 K the line shape is gaussian and the line width is almost constant, indicating that interactions of Li with surrounding atoms are constant and Li remains at times $\tau > (\langle\Delta\omega^2\rangle)^{-1/2}$ in fixed positions. $\langle\Delta\omega^2\rangle$ is the second moment of the spectrum recorded at low temperatures and can be calculated from the spin–spin relaxation time, with the expression: $\langle\Delta\omega^2\rangle = 2/(T_2)^2$. From the $1/T_2$ measured at low temperatures $\langle\Delta\omega^2\rangle = 4.25 \times 10^7\ \mathrm{s}^{-2}$ has been deduced [17]. Since the linewidth of the spectrum must be mainly due to dipole interactions, the second moment can be used to estimate the average Li–Li distance through Van Vleck's expression for a rigid lattice [22]. On the basis of a random distribution of lithium on A sites, 0.37 nm was obtained [17], which is close to the distance between the A sites of the perovskite structure ($a_p = 0.38$ nm).

At temperatures higher than 200 K, the line shape becomes Lorentzian and the line width decreases as a consequence of Li motion. In this case, the local fields are changing with time and only an averaged lithium interaction with its environment is observed. Cancellation of dipole interaction happens when the correlation time for Li motion, is smaller than $(\langle\Delta\omega^2\rangle)^{-1/2}$ (motional narrowing effect).

Results obtained for the temperature dependence of the spin-lattice relaxation rate, $1/T_1$, at frequencies of 10, 20 and 31 MHz, are displayed in Fig. 6. The rate, $1/T_1$, is related to the SLR relaxation function through the equation

$$\frac{1}{T_1(\omega_L, T)} = C\left[J'(\omega_L, T) + 4J'(2\omega_L, T)\right], \qquad (4)$$

where the spectral density function, $J(\omega)$, is the Fourier transform of the SLR relaxation function,

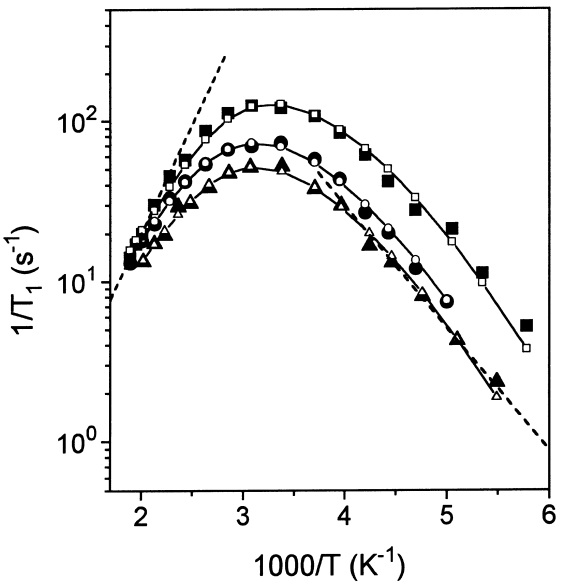

Fig. 6. Temperature dependence of $1/T_1$ at 10.6 MHz (■), 20 MHz (●) and 31 MHz (▲). Dashed lines have slopes of 0.26 eV at high temperatures and 0.15 eV at low temperatures. Open symbols are theoretical values for $1/T_1$ obtained from experimental conductivity data at the same frequencies. Lines connecting these symbols are guides for the eye.

C is a constant depending on the nuclear interaction responsible for the relaxation process and ω_L is the Larmor frequency.

The asymmetry of $1/T_1$ peaks results from a non-exponential relaxation function of the KWW form, $C(t) = \exp(-(t/\tau_s)^{\beta_s})$. According to Ngai's coupling model, activation energies, E_s and E_a, are defined such that E_s is an activation energy for long range motion and E_a is a microscopic activation energy free of the effect of cooperativity. On the base of a thermally activated relaxation mechanism, E_s and E_a are directly obtained from the slopes of the high and the low temperature sides of the $1/T_1$ plot, respectively, and both energies are related through the β exponent according to $E_a = \beta_s E_s$. However, in the case of a non-Arrhenius relaxation process, activation energies for ionic motion depend on temperature and the relation $E_a = \beta_s E_s$ holds only if both energies are calculated in the same temperature range. Experimental $1/T_1$ curves obtained for $Li_{0.5}La_{0.5}TiO_3$ show an activation energy $E_a = 0.15 \pm 0.0$ eV at low temperatures. The activation energy for the high temperature side of the peak cannot be estimated unambiguously except for data measured at 10 MHz, where a value of $E_s = 0.26$ eV is obtained. The value of β_s can be obtained from the frequency dependence of the $1/T_1$ in the low temperature side of the peaks at a given temperature, yielding the same 0.4 value for β_s provided the relation $1/T_1(\omega_L) \propto \omega_L^{-(1+\beta_s)}$ holds (see Fig. 4).

4. Discussion, comparison of SLR and ECR results

In the same temperature range where $E_s = 0.26$ eV was obtained from $1/T_1$ data at 10 MHz, an activation energy $E_\sigma = 0.26$ eV was also obtained from conductivity measurements, which we suggest shows that long range activation energies might be the same if they are measured at the same temperature. At low temperatures an activation energy for long range motion, $E_\sigma \sim 0.4$ eV, was obtained from dc conductivity data. The corresponding SLR activation energy, E_s, at low temperatures, can be obtained using Ngai's model. Since the activation energy obtained from the low temperature branches of $1/T_1$ curves is $E_a = 0.15$ eV, and β_s is 0.4, $E_s = E_a/\beta_s = 0.15/0.4 \cong 0.38$ eV, which is close to the energy found from conductivity data in the same temperature range. Therefore, the non-Arrhenius dependence of the relaxation time is also found from SLR measurements.

The above reasoning suggests that relaxation functions governing SLR and ECR might be actually the same, and in that case $1/T_1$ plots should be reproduced from conductivity measurements [21]. The Fourier transform of the ECR relaxation function can be rewritten as

$$\hat{\Phi}(\omega) = \frac{1}{\sigma^*(\omega)/\varepsilon_\infty + j\omega} = \frac{1}{(\sigma^*(\omega)/\sigma_{dc})\omega_p + j\omega}. \quad (5)$$

In an ideal Debye case, $\sigma^*(\omega) = \sigma_{dc}$, and the ECR rate is $\sigma_{dc}/\varepsilon_\infty$. But in the general case of a frequency dispersive conductivity there is a "frequency dependence" for the effective relaxation rate of the form $\sigma^*(\omega)/\varepsilon_\infty$. The spectral density function, $J(\omega)$, can be expressed in the same form as $\hat{\Phi}(\omega)$, but with a different relaxation rate. The NMR rate is given by the mean jump rate of the mobile ions, γ, which is connected to the ECR rate through the expression $\sigma_{dc} = \varepsilon_\infty(T_0/T)\gamma$. T_0 can be approximated by $T_0 = (nq^2x_0^2)/(6k_b\varepsilon_\infty)$, where n is the mobile ions concentration, q their charge, x_0 their hopping distance, and k_b the Boltzmann's constant. The calculated T_0 for this compound is 135 K. The attempt frequency obtained from the high temperature extrapolation of the mean jump rate of lithium ions, γ, turns out to be in the order of 10^{12} s^{-1}, which is in the range of typical phonon frequencies.

Therefore the $1/T_1$ rates can be calculated using, directly, experimental conductivity data according to expression (4) where the spectral density function takes the form

$$J(\omega) = \frac{1}{(\sigma^*(\omega)/\varepsilon_\infty)(T/T_0) + j\omega} = \frac{1}{(\sigma^*(\omega)/\sigma_{dc})\gamma + j\omega}. \quad (6)$$

Theoretical $1/T_1$ curves obtained from electrical conductivity results are compared with experimental $1/T_1$ data in Fig. 6. $1/T_1$ plots at 20 and 31 MHz have been calculated using extrapolated con-

ductivity values at 40 and 62 MHz according to expression (1). The good agreement found with experimental $1/T_1$ data supports the hypothesis that both SLR and ECR processes are governed by relaxation functions with the same β exponent and equally activated relaxation times. It is worth noting, however, that relaxation times differ in the preexponential factor. In fact, relaxation times obtained from the maxima of Figs. 3 and 6 using the relation $\omega\tau = 1$ are related through $\tau_\sigma(T) = (T/T_0)\tau_s(T)$. Discrepancies between relaxation times obtained from ECR and SLR measured in the same frequency range have been previously observed in glassy materials [11]. Finally, we remark that there is an interesting similarity between data obtained for a crystalline system and those obtained for glassy materials (KWW decay functions for the relaxation process and the non-Arrhenius temperature dependence of the conductivity and consequently of the relaxation time). The temperature dependence of the dc conductivity can be fitted to an empirical Vogel–Fulcher–Tamman (VFT) function of the form $\sigma_{dc} = \sigma_\infty \exp[-A/(T - T_K)]$ which is usually applicable in glasses above the glass transition temperature (continuous line in Fig. 2 corresponds to this fitting with $A = 1990$ K and $T_K = 73.3$ K). VFT function might phenomenologically account for the saturation effects predicted by the coupling model [13]. In fact, if A is regarded as an activation energy in the high temperature limit, 0.17 eV is obtained (see inset in Fig. 2) which is close to the microscope activation energy of 0.16 eV obtained from SLR and ECR at low temperatures. Moreover, dynamical measurements (permittivity, specific heat, viscosity) on many glass forming supercooled liquids and polymers show also non-Debye dependence of the susceptibility on frequency (and the KWW has been often proposed to fit the data), and relaxation times growing with decreasing temperatures faster than in a thermally activated process usually following VFT functions [22–24]. Glass like properties in crystalline ion conducting solids could be related to positional disorder in the mobile ions sublattice, i.e., a disordered configuration of Li ions in which all Li sites cannot be regarded as equivalent. However, additional work should be done to establish this point.

5. Conclusions

In summary, we have analyzed ECR and SLR in $Li_{0.5}La_{0.5}TiO_3$ in the same frequency and temperature range, showing that dc conductivity has a non-Arrhenius dependence, which is also observed from SLR measurements. This non-Arrhenius dependence is similar to that recently reported for many glassy ionic conducting materials. On the basis of the non-Arrhenius temperature dependence of the relaxation time, both relaxations can be described by equally stretched KWW relaxation functions. Relaxation times show the same VFT activated behavior but differ in the preexponential factors. In presence of this non-Arrhenius temperature dependence of the relaxation times it is important that ECR and SLR be compared over the same frequency and temperature ranges, otherwise "apparent" discrepancies can arise in the information extracted from both techniques.

References

[1] F. Borsa, D.R. Torgeson, S.W. Martin, H.K. Patel, Phys. Rev. B 46 (2) (1992) 795.
[2] K.L. Ngai, Phys. Rev. B 48 (18) (1993) 13481.
[3] R. Kohlrausch, Ann. Phys. Lpz. 72 (1847) 393.
[4] K.L. Ngai, Comments Solid State Phys. 9 (1979) 121; 9 (1980) 141; for a recent review see K.L. Ngai, in: R. Richert, A. Blumen (Eds.), Effects of Disorder on Relaxational Processes, Springer, Berlin, 1994, p. 89.
[5] K.L. Ngai, R.W. Rendell, H. Jain, Phys. Rev. B 30 (1984) 2133.
[6] S.R. Elliott, A.P. Owens, Phil. Mag. B 60 (6) (1989) 777.
[7] S.R. Elliott, A.P. Owens, Phys. Rev. B 44 (1) (1991) 47.
[8] K. Funke, Prog. Solid State Chem. 22 (1993) 111.
[9] M. Meyer, P. Maass, A. Bunde, Phys. Rev. Lett. 71 (4) (1993) 573.
[10] M. Tatsumisago, C.A. Angell, S.W. Martin, J. Chem. Phys. 97 (9) (1992) 6968.
[11] O. Kanert, R. Küchler, K.L. Ngai, H. Jain, Phys. Rev. B 49 (1) (1994) 76.
[12] J. Kincs, S.W. Martin, Phys. Rev. Lett. 76 (1) (1996) 70.
[13] K.L. Ngai, A.K. Rizos, Phys. Rev. Lett. 76 (8) (1996) 1296.
[14] Y. Inaguma, L. Chen, M. Itoh, T. Nakamura, T. Uchida, M. Ikuta, M. Wakihara, Solid State Commun. 86 (1993) 689.
[15] Y. Inaguma, L. Chen, M. Itoh, T. Nakamura, Solid State Ionics 70&71 (1994) 196.
[16] M. Itoh, Y. Inaguma, W. Jung, L. Chen, T. Nakamura, Solid State Ionics 70&71 (1994) 203.

[17] C. León, M.L. Lucía, J. Santamaría, M.A. París, J. Sanz, A. Várez, Phys. Rev. B 54 (1) (1996) 183.
[18] E. Fukushima, S. Roeder, Experimental Pulse NMR: A Nuts and Bolts Approach, Addison–Wesley, New York, 1981.
[19] C. León, M.L. Lucía, J. Santamaría, Phys. Rev. B 55 (1) (1997) 882.
[20] C. León, M.L. Lucía, J. Santamaría, Phil. Mag. B 75 (5) (1997) 629.
[21] K. Funke, D. Wilmer, Europhys. Lett. 12 (4) (1990) 363.
[22] N. Menon, S.R. Nagel, D.C. Venerus, Phys. Rev. Lett. 73 (7) (1994) 963.
[23] P.K. Dixon, S.R. Nagel, Phys. Rev. Lett. 61 (3) (1988) 341.
[24] R.D. Deegan, S.R. Nagel, Phys. Rev. B 52 (8) (1995) 5653.